

# Numerical Simulation of Wave Propagation in Mortar with Inhomogeneities

by Dimitrios G. Aggelis and Shouhei Momoki

*In this paper, wave propagation in concrete with inhomogeneity is examined using numerical simulations. Simulated damage is film-shaped to resemble the actual shape of cracks. Results of pulse velocity and wave distortion are compared with experimental ones, showing good agreement. It is concluded that, apart from the volume content, the characteristic shape and orientation of damage are crucial for wave propagation influencing the correlations between velocity and damage.*

**Keywords:** damage assessment; dispersion; nondestructive testing; pulse velocity; simulation.

## INTRODUCTION

Pulse velocity is a feature used for concrete characterization. It produces rough but valuable correlations with strength.<sup>1</sup> A more accurate characterization, however, is highly demanded because pulse velocity is not always sensitive to damage.<sup>2</sup> Wave dispersion parameters have recently been used for better characterization of cementitious materials.<sup>3-6</sup> The term “dispersion” is used to describe the velocity dependence on frequency. It has been seen, despite the fact that short wavelengths are more influenced in terms of attenuation by the presence of inhomogeneity, that propagation velocity increases with frequency. Phase velocity has been measured in material with actual microcracking due to freezing-and-thawing cycles and spherical polystyrene inclusions that simulate damage.<sup>3</sup> Frequency-dependent phase velocity has also been measured in actual concrete bridge decks to provide more accurate characterization capabilities concerning the repair of cracks.<sup>4</sup> Similar velocity-increasing trends have been found in cementitious material containing film-shaped inclusions in through-the-thickness<sup>5</sup> or surface mode.<sup>6</sup> Therefore, except for the velocity itself, the velocity-versus-frequency curve or velocity change with frequency could be used for a more accurate characterization.

Using scattering models,<sup>7,8</sup> accurate predictions can be made that explain the velocity dependence on frequency. However, they consider the spherical shape of inclusions.<sup>3,9</sup> The effort should continue in the direction of a more accurate simulation of the actual damage shape. Although this can be done in the experimental measurements (using different shapes of inclusions<sup>5,6</sup>), theoretical solutions are much more difficult for shapes other than spherical.

In the present paper, numerical simulation results are compared with experimental ones. Specifically, attention is focused on the waveform distortion caused by the presence of scatterers, the pulse velocity decrease, and the influence of different frequency. Different contents of inclusions from 0 to 10% are simulated. The shape is film-like to resemble actual crack topology. Therefore, orientation is also important. Some basic cases are examined additionally to the classic case of spherical inclusions, which is generally considered

easier and quite representative because of the possibly random orientation of the actual cracks.<sup>3</sup> The theoretical results support the frequency dependence of velocity and show that the shape and orientation of damage is equally important to the content. Additionally, the theoretical simulation allows expanding to cases that are difficult to simulate experimentally.

## RESEARCH SIGNIFICANCE

In nondestructive testing of concrete, it is important to develop new parameters to help in the diagnosis of flaws and deterioration; the study of stress wave velocity at different frequencies is a potential parameter that may assist in material characterization. This is because it has been experimentally shown that pulse velocity actually depends on the pulse frequency. Although this dependence has started to be studied, so far the trends have not been confirmed by theoretical results concerning the actual flaky shape of the cracks. In this paper, cracks are simulated by thin rectangular inclusions to produce realistic results. It is seen that the shape and orientation of cracks is an also important parameter besides their content. In addition, numerical simulations offer insight to cases that are difficult or impossible to examine experimentally and help establish correlations with damage.

## EXPERIMENTAL DETAILS

The specimens used for the experimental part were cubes with edges of 150 mm (5.900 in.). The mortar had a water-cement ratio ( $w/c$ ) of 0.5 by mass and a sand-cement ratio of 3 by mass. The maximum sand size was 2 mm (0.079 in.), significantly smaller than the inclusions. The inclusions were vinyl plates 15 x 15 x 0.5 mm (0.590 x 0.590 x 0.020 in.). They were placed during mixing of the materials at volume contents of 1, 5, and 10%. Measurements were conducted with different frequency tone-bursts of 10 cycles with central frequencies of 10, 30, 50, 80, 100, and 150 kHz to examine the propagation of different bands. Additionally, the form of one cycle was used to excite a broadband signal. The study focuses more at lower frequencies because higher frequencies are not suitable for in-place application due to concrete damping. More details about the experimental procedure can be found in References 5 and 6.

## NUMERICAL SIMULATION

The simulations were conducted with commercially available software.<sup>10</sup> It operates by solving the two-dimensional

ACI Materials Journal, V. 106, No. 1, January-February 2009.

MS No. M-2007-376.R1 received May 3, 2008, and reviewed under Institute publication policies. Copyright © 2009, American Concrete Institute. All rights reserved, including the making of copies unless permission is obtained from the copyright proprietors. Pertinent discussion including authors' closure, if any, will be published in the November-December 2009 ACI Materials Journal if the discussion is received by August 1, 2009.

**Dimitrios G. Aggelis** is an Assistant Professor in the Materials Science and Engineering Department, University of Ioannina, Ioannina, Greece. He received his Diploma in mechanical engineering and his PhD in nondestructive testing of concrete from the University of Patras, Patras, Greece. His research interests include concrete damage characterization using stress wave propagation techniques.

**Shouhei Momoki** is a Research Engineer at the Research Institute of Technology, Tobishima Corporation, Noda, Japan. He received his master's degree in agricultural engineering from the University of Kyoto, Kyoto, Japan. His research interests include damage monitoring and structural health condition evaluation of civil structures using nondestructive testing.

(2D) acoustic (elastic) wave equations based on a method of finite differences.<sup>11,12</sup> In this case, all materials were considered elastic with no viscosity components. Materials and geometry were set similar to the experiment. The material properties used for mortar were first and second Lamé constants  $\lambda_m = 10$  GPa (1450 ksi) and  $\mu_m = 15$  GPa (2176 ksi), respectively, and density  $\rho_m = 2300$  kg/m<sup>3</sup> (144 lb/ft<sup>3</sup>), whereas for the vinyl inclusions,  $\lambda_i = 1.7$  GPa (247 ksi),  $\mu_i = 1.15$  GPa (167 ksi), and  $\rho_i = 1200$  kg/m<sup>3</sup> (75 lb/ft<sup>3</sup>). The corresponding longitudinal velocities were  $C_m = 4170$  m/s (13,681 ft/s) and  $C_i = 1800$  m/s (5906 ft/s) for the mortar matrix and inclusions, respectively. It is noted that the actual cracks exhibit zero velocity. In this case, and to be able to compare the simulation results with the experimental results, however, it was deemed necessary to use mechanical property values close to the actually used inclusions. The specimen geometry was a square of 150 mm (5.900 in.) side and displacement excitation was introduced on one side. The simulated transducer and receiver were 15 mm (0.590 in.) long to resemble the actual transducers used in the experiment<sup>5,6</sup> and were placed on opposite sides of the geometry, that is, the distance was 150 mm (5.900 in.) (refer to Fig. 1). The receiver computed the average lateral displacement on its defined length.

The possible combinations of shapes, sizes, orientations, and concentrations of inclusions are limitless. The simulations

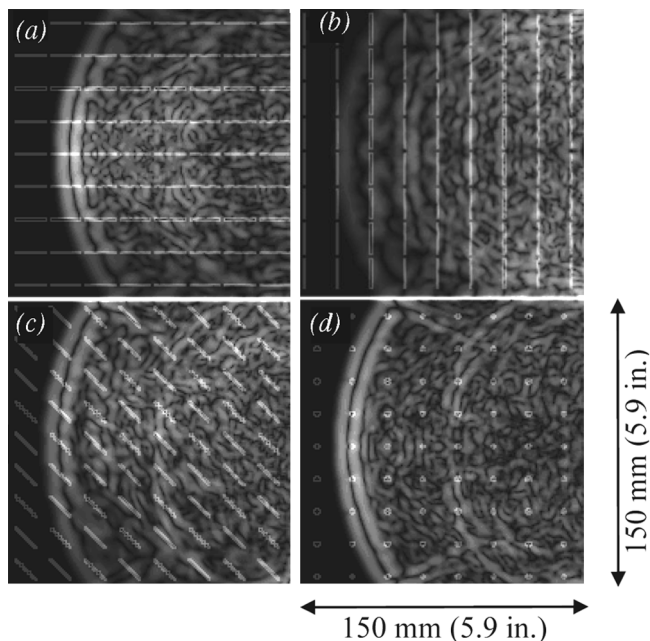


**Fig. 1**—Displacement field for different arrangement of inclusions relative to the propagation direction: (a) parallel; (b) vertical; (c) diagonal (45 degrees); and (d) spherical inclusions. The content is 1% by area. White color corresponds to high amplitude. The excitation (one cycle of 300 kHz) was introduced from the right.

presented herein were performed using the inclusions shape similar to the cross section of the experimentally used one, specifically 15 x 0.5 mm (0.590 x 0.020 in.), neglecting the third dimension of 15 mm (0.590 in.) of the actual inclusions to reduce the problem to two dimensions. Some extreme cases of orientation were tested, namely parallel and vertical to the propagation, as seen in Fig. 1(a) and (b). The case of 45-degree orientation was examined (refer to Fig. 1(c)) and the classic case of spherical inclusions is depicted in Fig. 1(d). The radius was 2 mm (0.079 in.), allowing each sphere to occupy a cross section area of the same order with each rectangular inclusion. It will be shown that the orientation played a fundamental role, even more important than the content itself.

One set of simulations was conducted with the excitation of one cycle of 300 kHz to mainly study the effect of inclusions on the waveform distortion and pulse velocity. Another set was conducted with 10 cycles of different central frequencies, namely 10, 30, 50, 80, 100, and 150 kHz. The aim was to examine the effect of inclusions on the propagation velocity of different frequency pulses and compare with corresponding experimental results.

After some trials, the spacing resolution was set to 0.2 mm (0.008 in.). Even for the highest frequency used (300 kHz), the wavelength was approximately 13 mm (0.512 in.). This shows that there were at least six points per cycle that could be considered an adequate depiction. Additionally, the indicative simulations using spacing of 0.1 mm (0.004 in.) resulted in exactly the same calculated pulse velocity, though were more time consuming.

## RESULTS

In Fig. 1, besides the arrangement of the inclusions, one can see the visualization of the displacement field, approximately 30  $\mu$ s after the 300 kHz one-cycle excitation. All four cases concern inclusion content of 1% by cross section area. It can be confirmed by visual observation of the displacement field that the case of inclusions vertical to the propagation (Fig. 1(b)) causes the strongest distortion of the wavefront. This is reasonable because a significant part of the energy is reflected back at each encounter by the large surface of the perpendicular inclusions. The parallel case (Fig. 1(a)) does not influence the forward direction much, whereas the spherical shape (Fig. 1(d)) seems to influence the propagation at any angle less. It is also seen that when the size of the obstacle face (side perpendicular to the wavefront) is similar to the major wavelength of 13 mm (0.512 in.) (refer to Fig. 1(b)) with an inclusion face of 15 mm (0.590 in.), the pattern is substantially distorted, whereas for the case of parallel-to-propagation inclusions (perpendicular side of 0.5 mm [0.020 in.]) and spherical inclusions of 2 mm (0.079 in.) radius, the forward direction is not greatly affected (refer to Fig. 1(a) and (d), respectively). It is interesting to note that for the diagonal case (Fig. 1(c)), the wave front shows a preference according to the angle of the inclusions.

The waveform recorded at the receiver is different for any of the aforementioned cases. Before presenting the simulated waveforms, it is worth seeing typical experimental waveforms collected at the actual material with inclusions. Typical waveforms for plain mortar, mortar with 5 and 10% of inclusions, are depicted in Fig. 2. One observation concerns the cycle duration. As the inclusion content increases, it seems that the pulse becomes wider. This has been attributed to the distribution of energy to several possible propagation

paths, each one resulting in different transit times.<sup>6</sup> This practically results in a frequency downshift and, therefore, strong attenuation of the higher frequencies.<sup>5</sup>

Examples of waveforms resulting from the numerical simulation can be seen in Fig. 3. The first case (Fig. 3(a)) concerns spherical inclusions. It is confirmed that inhomogeneity distorts the waveform. It seems that the energy that was concentrated in the first cycle in the homogeneous material is spread to a longer duration for 5 and 10% of the inclusions, as was the case for the experimental waveforms of Fig. 2. The same holds for the case of inclusions parallel to propagation (refer to Fig. 3(b)). For diagonal and perpendicular inclusions, the waveforms lose a lot of energy (thus they are presented magnified) and the cycles become obviously longer (refer to Fig. 3(c) and (d), respectively), cutting off higher frequencies. From the aforementioned simulations, it can be concluded that the waveforms from spherical inclusions and the parallel-to-propagation arrangement of thin inclusions seem closer to the actually recorded waveforms, depicted in Fig. 2.

### Pulse velocity

The shape distortion discussed previously was the first effect of inhomogeneity. This influenced the measured parameters, such as the pulse velocity. Figure 4 shows the velocities of the propagating pulses for different content and arrangement of inclusions, measured by the leading edge of the waveforms of Fig. 3. It is seen that the velocity decreased for any different kind of scatterer, with the spherical case exhibiting the smallest decrease (5.5% for 10% inclusion volume content). The largest decrease was observed by the vertical inclusions (more than 30%), whereas the parallel case resulted in a 12% decrease for the maximum damage content examined. The experimental results of the previous study<sup>5</sup> were quite close to the parallel case. It was also seen that the spherical case resulted in a higher velocity than the experimental and the simulations with any other arrangements of inclusions. Therefore, it seems that simulations should not be restricted to the spherical size because the actual shape of damage was different and resulted in lower velocities. In any case, it was seen that the percentage of pulse velocity drop was of the same order with the damage content (approximately 10%) except for the extreme case of damage pattern vertical to the propagation direction, which in actual cases is highly unlikely. This slight velocity decrease was indicative but not satisfactory to characterize all cases. Therefore, more sensitive parameters were required, which led to the dispersion study that follows.

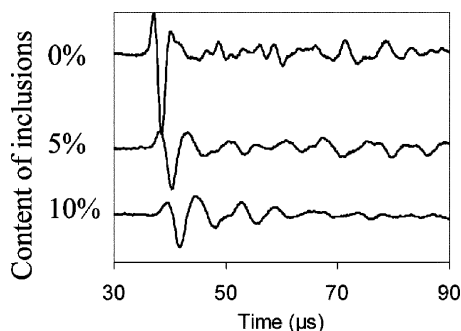


Fig. 2—Experimental waveforms from mortar with different content of inclusions.

### Dispersion

The waveform distortion was mainly a result of the fact that different frequencies propagate with different velocities. The frequency dependence of velocity was measured in many composite systems<sup>13-15</sup> as well as concrete<sup>3-6,9,16-18</sup> and can be theoretically supported by scattering models.<sup>3,9,18</sup> The size and the arrangement of scatterers (inclusions or cracks) influence each propagating wavelength in a different way.<sup>7,8</sup>

In the previous experimental study,<sup>5</sup> it was found that the velocity, measured by the transit time of the leading edge of the waveform (10 sinusoidal cycles), exhibited a slight increase as the frequency of the pulse increased from 10 to 150 kHz. These velocity results are depicted in Fig. 5(a). The increase of pulse velocity throughout this frequency band was higher for 10% of the damage. Specifically, for sound material, the velocity increased from 4081 to 4131 m/s (13,389 to 13,553 ft/s) (an increase of 1.22%). Concerning the heavily damaged material (with 10% inclusions), the increase was from 3463 to 3580 m/s (11,361 to 11,745 ft/s) (or 3.37%). This shows that the dispersion increased by a factor of approximately 3 compared with the healthy material while, at the same time, the pulse velocity itself reduced by only approximately 10%, as seen in Fig. 4.

Similar trends measured previously<sup>5</sup> were explained with the scattering theory using the spherical shape approximation. In the present study, the simulation results were conducted with the actual size of the inclusions, as mentioned previously, therefore, being more accurate.

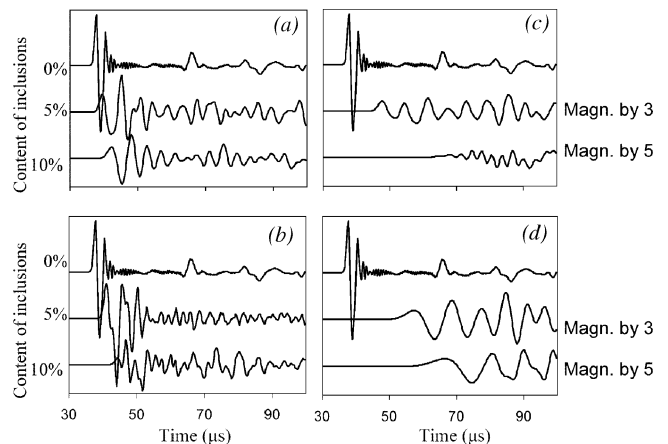


Fig. 3—Numerically obtained waveforms for different inclusion content: (a) spherical inclusions; (b) rectangular inclusions parallel to propagation; (c) diagonal; and (d) perpendicular.

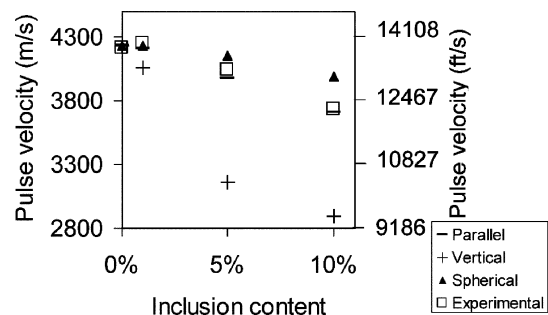


Fig. 4—Pulse velocity versus inclusion content for different cases of orientation.

In Fig. 5(b), velocities measured from simulated waveforms with respect to the parallel arrangement of the thin inclusions and different volume contents are depicted. The increasing trend of velocity is obvious in this case too. The perpendicular orientation (Fig. 5(c)) resulted in much lower velocities, even less than 3000 m/s (9842 ft/s) for 10% damage. Finally, the spherical shape case, which is depicted in Fig. 5(d), resulted in the highest velocities, as was also seen previously for the broadband signal of 300 kHz. The aforementioned simulations confirm the experimentally observed dispersion, showing that, in inhomogeneous material, the velocity is expected to rise with frequency. Except for concrete, this has been observed in studies concerning different composite materials.<sup>13-15,18</sup>

While short wavelengths exhibit higher propagation velocities, they are more influenced in terms of amplitude. An example is depicted in Fig. 6, where the initial part of waveforms of 30 and 500 kHz are depicted. The waveforms concern simulation with the vertical arrangement of inclusions. It is obvious that the 500 kHz is of much lower amplitude. Additionally, the results of Fig. 6 indicate that the leading edge of the 500 kHz waveform arrives approximately 1  $\mu$ s earlier.

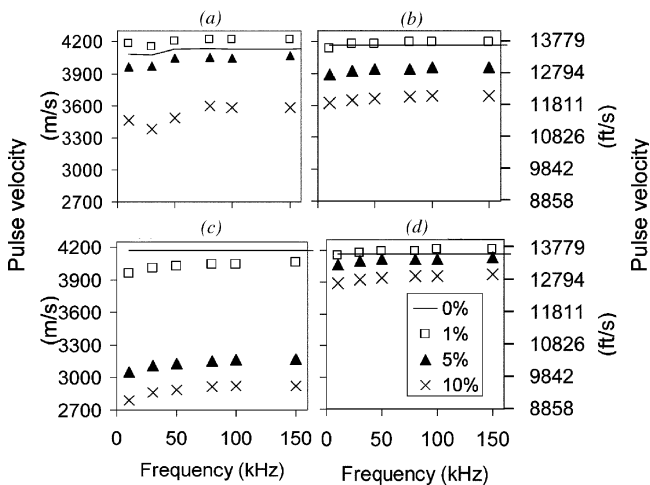


Fig. 5—Pulse velocity of mortar with different inclusion contents versus frequency: (a) experimental and theoretical for different cases of inclusions; (b) rectangular parallel to propagation; (c) rectangular perpendicular; and (d) spherical.

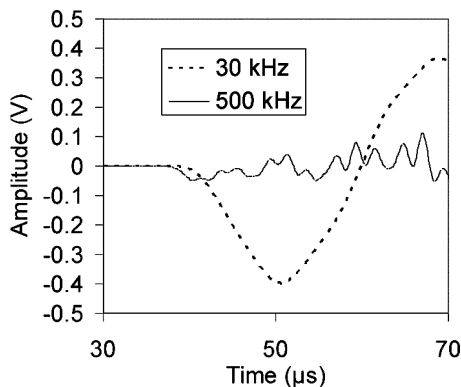


Fig. 6—Leading edge of received waveforms for different frequencies through mortar with 1% of inclusions vertical to the wave propagation (simulation results). The waveform of 500 kHz is magnified by two for clarity.

Numerical simulations after solution of the wave equation enlighten the problem at hand. It is still difficult, however, to use a simple way to explain the phenomenon of velocity dispersion without the risk of being simplistic. One possible simple explanation could be the following: in the case of short wavelengths, apart from the energy that is scattered by the inclusions, some part of it actually travels through the stiff matrix alone, therefore exhibiting higher velocity. On the other hand, long wavelengths (longer than the inclusions) propagate through the homogenized volume of matrix with embedded soft inclusions, therefore having inferior effective properties. This homogenized volume has reduced mechanical properties compared with the stiff matrix. Therefore, long wavelengths exhibit lower velocities than short ones.

As was seen previously, the dispersive trend (increase of velocity with pulse frequency) becomes stronger with the inclusion content. This is presented in Fig. 7, where the increase of velocity between 10 and 150 kHz is depicted versus the inclusions' content for different configurations of the inclusions, along with the experimental results. The increase of velocity throughout this band is higher for the vertical arrangement of the inclusions, namely 4.8%. It is again seen that the spherical case is closer to the parallel than the vertical case, while the experimental dispersion is slightly higher (3.1%). As to the experiment, dispersion could be measured even for plain mortar. Mortar is by itself inhomogeneous because it contains sand grains and porosity (even though of small size). In the simulation, however, the matrix was considered homogeneous and therefore the dispersive behavior of plain mortar was not numerically examined. The observed dispersion of the results was due to the simulated damage alone.

It can be concluded that, as the inhomogeneity increases, the velocity decreases for any frequency, whereas the dispersion increases. This is reasonable because inhomogeneity is the source of dispersion and, therefore, an increase in its content results in more highlighted dispersive effects. The significance is that the use of different frequencies will enhance the discrimination between homogeneous and inhomogeneous material because the dispersion (or the increase of velocity) throughout the low frequency band up to 150 kHz seems very sensitive to the existence of damage. For the experimental case, the dispersion of material with 10% simulated damage was approximately three times (300%) that of sound material, as seen in Fig. 7. The same trend holds for the different numerically simulated cases, showing that dispersion was more sensitive than pulse velocity itself that exhibits only a

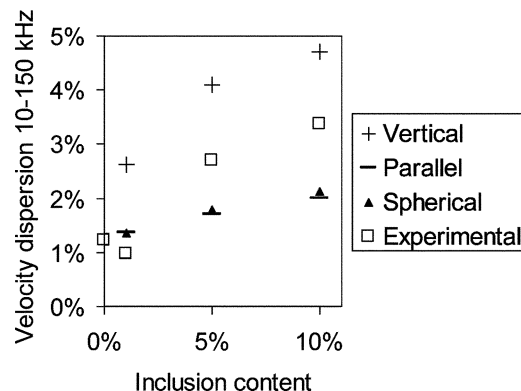


Fig. 7—Increase of velocity between 10 and 150 kHz for different inclusion contents and arrangements of inclusions.

slight decrease, even for high damage percentage. Practically, to examine the dispersion of concrete, velocity measurements should be done at low frequencies (suggested 10 kHz) and higher (150 kHz). In case the velocity difference between the two frequencies is high (approximately 200 m/s [656 ft/s]) this will imply strong inhomogeneity, whereas if the velocities at 10 and 150 kHz are similar (within 50 m/s [164 ft/s]), this implies sound material.

The explanation of a phenomenon as complicated as wave dispersion in a medium as heterogeneous as concrete is a very difficult task. It is believed, however, that the difficulty should not discourage study, both experimentally and numerically, because a lot of new information can result and hopefully interesting and robust correlations between wave parameters and material quality can be established.

## CONCLUSIONS

In the present paper, wave propagation in inhomogeneous cementitious material was numerically simulated. Inclusions were film-shaped to realistically resemble the actual cracks. The inclusions had a significant influence on the waveform shape and the pulse velocity measured by the arrival of the leading edge. Additionally, tone bursts of different central frequencies revealed the dispersive nature of the material because the propagation velocity increased with frequency. The aforementioned results were compared with recent experimental ones, showing good agreement.

The basic conclusions are summarized as follows:

1. Inhomogeneity results in lower wave velocity and higher dispersion (velocity dependence on frequency);

2. Dispersion is a promising feature to study because it is a result of inhomogeneity and, therefore, exhibits much higher sensitivity to damage than pulse velocity itself. It is reminded that pulse velocity in most cases experiences a change of less than 10% compared with the healthy material (refer to Fig. 4). Dispersion (velocity change between 10 and 150 kHz), however, increases by more than 200% compared again with that of the sound material (refer to Fig. 7);

3. The damage content is not the only important parameter; shape and orientation of cracks can also affect wave parameters to a great extent. This shows that damaged concrete does not behave as a homogeneous material because the damage content is not enough to describe the propagation behavior;

4. The spherical shape of damage that has been used in previous cases as an appropriate simulation tends to overestimate the velocity compared with experimental results and the rest of the arrangements examined theoretically. Therefore, although it is a reasonable and easy approximation, it is suggested that, when possible, other shapes for damage should also be simulated; and

5. Simulations produce results close to the experimental results and help expand the understanding to cases that are difficult to study experimentally.

More detailed simulations will be carried out to better understand the behavior of the material. They should not

concern only the velocity of longitudinal waves. Attenuation, frequency content, and surface waves are other interesting possibilities to expand the study. Additionally, it would be useful to introduce a wider variety of crack shapes and viscosity components to account for the damping of concrete, except for the scattering losses.

## REFERENCES

1. Anderson, D. A., and Seals, R. K., "Pulse Velocity as a Predictor of 28- and 90-Day Strength," *ACI JOURNAL, Proceedings* V. 78, No. 2, Mar.-Apr. 1981, pp. 116-122.
2. Popovics, S., and Popovics, J. S., "Effect of Stresses on the Ultrasonic Pulse Velocity in Concrete," *Materials and Structures*, V. 24, 1991, pp. 15-23.
3. Chaix, J. F.; Garnier, V.; and Corneloup, G., "Ultrasonic Wave Propagation in Heterogeneous Solid Media: Theoretical Analysis and Experimental Validation," *Ultrasonics*, V. 44, 2006, pp. 200-210.
4. Aggelis, D. G., and Shiotani, T., "Repair Evaluation of Concrete Cracks Using Surface and Through-Transmission Wave Measurements," *Cement and Concrete Composites*, V. 29, 2007, pp. 700-711.
5. Aggelis, D. G., and Shiotani, T., "Effect of Inhomogeneity Parameters on Wave Propagation in Cementitious Material," *ACI Materials Journal*, V. 105, No. 2, Mar.-Apr. 2007, pp. 187-193.
6. Aggelis, D. G., and Shiotani, T., "Experimental Study of Surface Wave Propagation in Strongly Heterogeneous Media," *Journal of the Acoustic Society of America*, V. 122, No. 5, 2007, pp. 151-157.
7. Foldy, L. L., "The Multiple Scattering of Waves," *Physical Review*, V. 67, 1945, pp. 107-119.
8. Waterman, P. C., and Truell, R., "Multiple Scattering of Waves," *Journal of Mathematical Physics*, V. 2, 1961, pp. 512-537.
9. Aggelis, D. G.; Polyzos, D.; and Philippidis, T. P., "Wave Dispersion and Attenuation in Fresh Mortar: Theoretical Predictions vs. Experimental Results," *Journal of the Mechanics and Physics of Solids*, V. 53, 2005, pp. 857-883.
10. Wave2000, Cyber-Logic, Inc., NY, <http://www.cyberlogic.org>.
11. Luo, G.; Kaufman, J. J.; Chiabrera, A.; Bianco, B.; Kinney, J. H.; Haupt, D.; Ryaby, J.; and Siffert, R. S., "Computational Methods for Ultrasonic Bone Assessment," *Ultrasound in Medicine & Biology*, V. 25, No. 5, 1999, pp. 823-830.
12. Kaufman, J. J.; Luo, G.; and Siffert, R. S., "On the Relative Contributions of Absorption and Scattering to Ultrasound Attenuation in Trabecular Bone: A Simulation Study," *IEEE Ultrasonics Symposium*, 2003, pp. 1519-1523.
13. Kinra, V. K., and Rousseau, C., "Acoustical and Optical Branches of Wave Propagation," *Journal of Wave Material Interaction*, V. 2, 1987, pp. 141-152.
14. Cowan, M. L.; Beaty, K.; Page, J. H.; Zhengyou, L.; and Sheng, P., "Group Velocity of Acoustic Waves in Strongly Scattering Media: Dependence on the Volume Fraction of Scatterers," *Physics Review E*, V. 58, 1998, pp. 6626-6636.
15. Anson, L. W., and Chivers, R. C., "Ultrasonic Velocity in Suspensions of Solids in Solids—A Comparison of Theory and Experiment," *Journal of Physics D*, V. 26, 1993, pp. 1566-1575.
16. Popovics, S.; Rose, J. L.; and Popovics, J. S., "The Behavior of Ultrasonic Pulses in Concrete," *Cement and Concrete Research*, V. 20, 1990, pp. 259-270.
17. Philippidis, T. P., and Aggelis, D. G., "Experimental Study of Wave Dispersion and Attenuation in Concrete," *Ultrasonics*, V. 43, 2005, pp. 584-595.
18. Aggelis, D. G.; Tsinopoulos, S. V.; and Polyzos, D., "An Iterative Effective Medium Approximation (IEMA) for Wave Dispersion and Attenuation Predictions in Particulate Composites, Suspensions and Emulsions," *Journal of the Acoustic Society of America*, V. 116, No. 6, 2004, pp. 3443-3452.